RESEARCH PAPER

RNA Biology 10:8, 1345–1355; August 2013; © 2013 Landes Bioscience

# The 5'-3'exoribonuclease Pacman (Xrn1) regulates expression of the heat shock protein Hsp67Bc and the microRNA *miR-277–3p* in *Drosophila* wing imaginal discs

Christopher I Jones[1], Dominic P Grima[1], Joseph A Waldron[1], Sue Jones[2], Hannah N Parker[3], and Sarah F Newbury[1,*]

[1]Brighton and Sussex Medical School; Medical Research Building; University of Sussex; Falmer, Brighton, UK; [2]Information and Computational Sciences; The James Hutton Institute; Invergowrie, Dundee, UK; [3]School of Pharmacy; University of Nottingham; Nottingham, UK

**Keywords:** Pacman, Xrn1, RNA stability, RNA degradation, *Drosophila* development, imaginal discs, miRNAs, exoribonuclease, post-transcriptional control

Pacman/Xrn1 is a highly conserved exoribonuclease known to play a critical role in gene regulatory events such as control of mRNA stability, RNA interference, and regulation via miRNAs. Although Pacman has been well studied in *Drosophila* tissue culture cells, the biologically relevant cellular pathways controlled by Pacman in natural tissues are unknown. This study shows that a hypomorphic mutation in *pacman* (*pcm*$^5$) results in smaller wing imaginal discs. These tissues, found in the larva, are known to grow and differentiate to form wing and thorax structures in the adult fly. Using microarray analysis, followed by quantitative RT-PCR, we show that eight mRNAs were increased in level by > 2-fold in the *pcm*$^5$ mutant wing discs compared with the control. The levels of pre-mRNAs were tested for five of these mRNAs; four did not increase in the *pcm*$^5$ mutant, showing that they are regulated at the post-transcriptional level and, therefore, could be directly affected by Pacman. These transcripts include one that encodes the heat shock protein Hsp67Bc, which is upregulated 11.9-fold at the post-transcriptional level and 2.3-fold at the protein level. One miRNA, *miR-277-3p*, is 5.6-fold downregulated at the post-transcriptional level in mutant discs, suggesting that Pacman affects its processing in this tissue. Together, these data show that a relatively small number of mRNAs and miRNAs substantially change in abundance in *pacman* mutant wing imaginal discs. Since Hsp67Bc is known to regulate autophagy and protein synthesis, it is possible that Pacman may control the growth of wing imaginal discs by regulating these processes.

## Introduction

A key aspect in the regulation of eukaryotic gene expression is the cytoplasmic control of mRNA stability. The effect of controlled RNA turnover on gene expression can be extremely significant, for example, some studies have shown that 40–50% of changes in gene expression occur at the level of RNA stability.[1] In multicellular organisms, it is increasingly evident that degradation of specific mRNAs is critical for the regulation of many cellular processes, including early development, infection, and inflammation, apoptosis and aging.[2-5] For example, in mice deficient for the RNA-binding protein Tristetraprolin, the stability of RNAs such as *GM-CSF*, *TNF*-α, and *Interleukin-10* increases, resulting in a systemic inflammatory syndrome with autoimmunity and bone marrow overgrowth.[6-8] Therefore, transcript degradation can be selective and modulated, suggesting a little studied layer of control of gene expression affecting cellular processes.

This study focuses on *Drosophila* Xrn1 (Pacman), a 5'-3' cytoplasmic exoribonuclease that is highly conserved, with homologs in humans (XRN1), *C. elegans* (XRN-1), and *S. cerevisiae* (Xrn1p).[9-11] Pacman/Xrn1 has been shown to processively degrade mRNAs in a 5'-3' direction after they have been decapped.[2,12] Pacman is not only involved in the cytoplasmic turnover of RNA but is also required during RNA interference, degradation via miRNAs, and in nonsense-mediated decay.[13] Our data, and those of others, show that Pacman is enriched in dynamic cytoplasmic particles termed P-bodies (processing bodies) and is co-localized with many of the other enzymes in the 5'-3' pathway, including the decapping enzyme Dcp2, the decapping activator Dcp1, and the helicase Me31B (Dhh1/p54 in yeast/humans).[5,14-16] The crystal structure of the N-terminal region of Pacman has been determined at high resolution.[17] This structure reveals that the catalytic domain comprises a pocket of basic residues which interacts with the 5' phosphate of the RNA and positions the first nucleotide for cleavage. The RNA is then pulled through the narrow entrance to the active site by a Brownian ratchet mechanism. The C-terminal domain of the protein (from residues 1140–1612), is less conserved overall

*Correspondence to: Sarah F Newbury; Email: s.newbury@bsms.ac.uk
Submitted: 12/13/2012; Revised: 06/10/2013; Accepted: 06/10/2013
http://dx.doi.org/10.4161/rna.25354

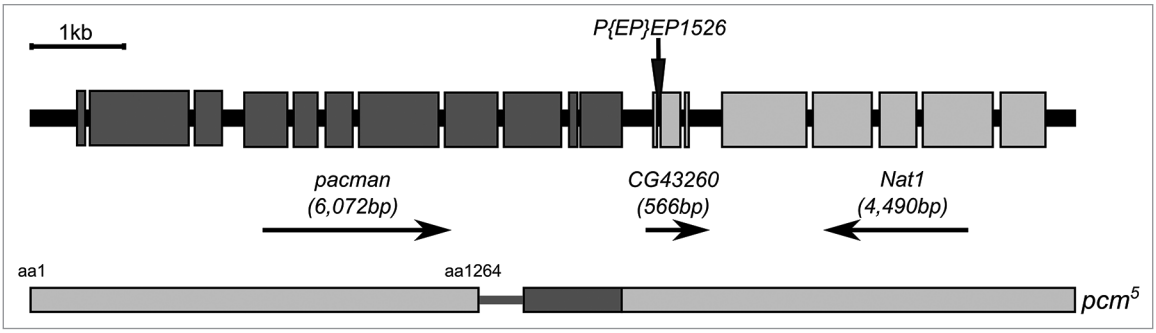


**Figure 1.** *pcm* genomic region and the allele *pcm*$^5$ created by imprecise excision of *P{EP}EP1526*. The *pacman* gene consists of 11 exons and expresses a single transcript. The *pcm*$^5$ allele is a 516 bp deletion in exons 8 and 9 with the rest of the gene sequence being out of frame (darker box). A "footprint" sequence of 32 bp remains in the position the P-element previously occupied, which is within the first intron of *CG43260*. *CG43260* is otherwise unaffected. Amino acid numbers indicate the region of Pacman protein not affected by the deletion in the *pcm*$^5$ allele (residues 1–1264 of 1612).

but does include some areas of conservation, termed short linear motifs (SliMs).[18] It has recently been shown that a short section of the C-terminal domain of Pacman (residues 1323–1355) interacts directly with the decapping factor Dcp1 and is required for efficient mRNA decapping in *Drosophila* S2 cells.[19]

Our previous work has shown that mutations in the *pacman* gene particularly affect growth and differentiation of tissues derived from the wing imaginal discs.[20] Formation of wing imaginal discs begins during embryogenesis and they then grow and differentiate during larval and pupal development to generate specific adult structures such as the thorax, wings, and sensory bristles. Imaginal discs have similarities to adult stem cells in that they have the capacity to differentiate into a number of specific cell types.[21] They therefore provide an excellent system for examining growth, differentiation, and specification of an adult tissue. Hypomorphic mutations in *pacman* (e.g., *pcm*$^5$) result in viable adults with a number of defects ,including dull wings, ruffling of the posterior wing margin, and bent or multiple sensory bristles.[20] When the copy number of *pcm*$^5$ is reduced from two to one by placing the hypomorphic allele over a deletion (e.g., *pcm*$^5$/*Df(1)JA27*), flies can have a cleft thorax phenotype where the wing imaginal discs have failed to seal together in a process similar to wound healing.[20] These specific phenotypes suggest that Pacman is likely to be degrading particular RNAs within wing imaginal discs.

To determine the mechanisms by which Pacman affects the development and differentiation of wing imaginal discs, it is first necessary to identify the RNAs misexpressed in this tissue in a *pcm* mutant. In this study, we report that a rather small number of mRNAs and miRNAs are substantially increased or decreased in levels in *pcm*$^5$ mutant discs. Of these misexpressed mRNAs, we have identified four that are upregulated at the post-transcriptional level in *pcm*$^5$ mutants, suggesting that they could be directly affected by the Pacman exoribonuclease. The upregulated transcripts include those associated with induction of autophagy and inhibition of protein synthesis. One miRNA, *miR-277-3p*, was post-transcriptionally downregulated, which is consistent with Pacman being specifically involved in the biogenesis of this miRNA. These data therefore suggest that Pacman controls growth of imaginal discs via control of protein synthesis and regulation of autophagy.

## Results

**The hypomorphic mutation in *pacman* (*pcm*$^5$) results in small wings and wing imaginal discs.** In order to determine the biological functions of Pacman, we previously generated a number of mutant alleles in the *pacman* gene, created by excision of a P-element downstream of *pacman*. The strongest hypomorphic allele generated, *pcm*$^5$ includes a partial deletion of exons 8 and 9, followed by a frameshift (**Fig. 1**). This results in a protein that includes the N-terminal catalytic domain (residues 1–674) but is missing residues 1264–1612 of the less structured C-terminal domain (residues 675–1612). Adult flies which are homo- or hemizygous for *pcm*$^5$ exhibit a number of phenotypes including dull wings (**Fig. 2**, panels A and B), duplicated macrochaetae and a cleft thorax,[20] suggesting that *pacman* affects the development of the wings from the wing imaginal disc. To further investigate the effect of *pacman* mutations on wing development, we measured the size of male *pcm*$^5$ wings and found them to be around 84% the size of wild-type wings (**Fig. 2**, panel C), while the average size (measured by weight) of wild-type and *pcm*$^5$ males did not vary (mean weight of control males = 1.02 mg (SD 0.10 mg, n = 23) and *pcm*$^5$ males = 0.98 mg (SD 0.10 mg, n = 23) compared using a t-test, p = 0.2069). To determine whether the decrease in wing size in mutants was due to smaller wing imaginal discs, the wing discs were dissected from wild-type and *pcm*$^5$ wandering L3 larvae and compared in size. The *pcm*$^5$ wing imaginal discs were found to be 82% the size of wild-type (**Fig. 2**, panel D). Therefore, this mutation in *pacman* appears to affect growth of the wing imaginal discs, presumably by affecting the expression of transcripts encoding proteins involved in development of that tissue.

**Relatively few transcripts are differentially expressed in *pcm*$^5$ wing imaginal discs.** In order to identify the mRNAs that change in abundance in the *pcm*$^5$ mutant and which therefore may result in reduced growth of the wing imaginal discs, we made use of Affymetrix *Drosophila* Genome 2.0 mRNA microarrays. A total of 960 wing imaginal discs were dissected from 3rd instar *pcm*$^5$ larvae and from wild-type controls and divided into four biological replicates for each genotype. This number of wing discs was sufficient to produce enough mRNA for the microarray

experiment and qRT-PCR validation experiments (> 4 μg). RNA extraction, labeling, array hybridization, and initial analyses were performed at the Sir Henry Wellcome Functional Genomics Facility, University of Glasgow. Quality control analysis of the raw data, performed using RMAExpress software,[22] showed that each array was of similar quality, with none falling outside the main intensity grouping. We analyzed the data from the mRNA microarray experiments using three different normalization methods: MAS5,[23] RMA,[22] and GCRMA.[24] Lists of differentially expressed genes were created after normalization with each method and then compared to identify genes that appeared consistently in at least two lists. These genes were predicted to be up or downregulated due to a real biological difference, rather than being false positives. Thirty-eight genes were found to be upregulated in *pcm*$^5$ wing imaginal discs (**Fig. 3**, panel A) and 34 genes were found to be downregulated (**Fig. 3**, panel B). We found that rather few mRNAs were expressed at levels greater than 1.5-fold in *pcm*$^5$ mutants compared with wild-type. Twenty-six mRNAs were upregulated more than 1.5-fold in these mutants, with only nine of these expressed at greater than 2-fold of the levels of controls. Of the 34 downregulated genes, 28 were below 1.5-fold and 16 below 2-fold. The *pacman* transcript itself was downregulated by 2.6-fold on the arrays, congruent with the 3-fold downregulation of the *pacman* transcript we have previously observed for *pcm*$^5$ mutant larvae.[2] Therefore, these data show, for the first time, than the *pcm*$^5$ mutation results in rather few transcripts which change in abundance at this stage of development in wing imaginal discs.

**Verification of microarray results using quantitative RT-PCR.** In order to validate the changes in transcript abundance in wing imaginal discs resulting from the *pcm*$^5$ mutation, TaqMan qRT-PCR was employed to determine the fold changes more precisely for a set of selected up and downregulated mRNAs. Twelve upregulated mRNAs were chosen for verification by qRT-PCR (the top 11 and the transcript encoding the decapping enzyme *Dcp2*), along with seven downregulated mRNAs (the six most downregulated and *pacman*). RNA levels were normalized to *rp49* (*RpL32*) mRNA as it did not change in level on the arrays and encodes a ubiquitously expressed ribosomal protein. Expression of each mRNA was tested on at least four biological replicates (up to 11, see **Fig. 4** legend). RNA from each biological replicate was converted to cDNA in duplicate and the qRT-PCR performed in duplicate on each cDNA sample (four technical replicates in total per biological replicate). **Figure 4** shows that the levels of transcripts, as measured by qRT-PCR, were comparable with the microarray levels in most cases. *CG31157* and *CG7966* appeared to be downregulated on the arrays, but were not found to differ in expression by qRT-PCR. Two other downregulated mRNAs, *CG17669* and *Dscam4*, were found to be downregulated by a much greater extent by qRT-PCR than they were on the arrays. Additionally, *Hsc70-2* appeared to be expressed extremely inconsistently at a very low level by qRT-PCR. *Hsc70-2* was not considered further, as the TaqMan assay may have been ineffective at detecting it (not shown). These qRT-PCR experiments showed that eight of the 12 upregulated mRNAs were increased in level by > 2-fold in

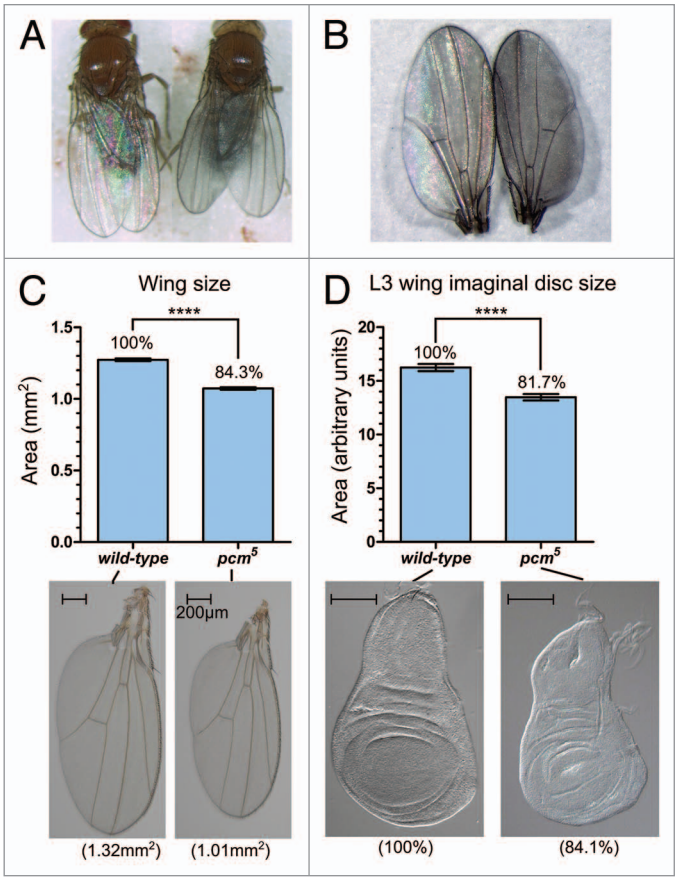


**Figure 2.** *pcm*$^5$ wing and wing imaginal disc phenotypes. (**A and B**) *pcm*$^5$ wings (right) frequently display a dull wing phenotype where the wild-type iridescence (left) is lost. (**C**) The wings of *pcm*$^5$ males are smaller than that of wild-type males. The mean wing area of *pcm*$^5$ males is 1.07 mm$^2$, 16% smaller than equivalent wild-type wings (1.27 mm$^2$). A t-test was used to calculate significance and error bars show standard error (n = 20 for wild-type and 21 for *pcm*$^5$ **** = p < 0.0001). Representative wild-type and *pcm*$^5$ wings are shown below (actual size in parenthesis). (**D**) The wing imaginal discs of *pcm*$^5$ L3 larvae are 18% smaller than those of wild-type discs. A t-test was used to determine significance and error bars show standard error (n = 32 for wild-type and 25 for *pcm*$^5$, **** = *P* < 0.0001). Representative wild-type and *pcm*$^5$ L3 wing discs are shown below (relative size in parenthesis).

the *pcm*$^5$ mutant compared with the control (*Hsp67Bc*, *CG31477*, *simjang*, *CG33099*, *Hsp26*, *CG5953 CG5326*, and *CG12842*). The *pacman*, *CG32364*, *CG17669*, and *Dscam4* transcripts were downregulated by > 2-fold (**Fig. 4**).

***Hsp67Bc*, *CG31477*, *simjang* and *Hsp26 transcripts* are post-transcriptionally upregulated in *pcm*$^5$ mutants.** Since mutations in *pacman* result in specific phenotypes, including reduced size of wing imaginal discs, we wished to concentrate on transcripts that changed significantly in abundance in the *pcm*$^5$ mutant compared with controls. We reasoned that these are most likely to result in the phenotypic consequences observed. Since Pacman is an exoribonuclease, and is involved in the degradation of RNA, we reasoned that transcripts upregulated at the mRNA level, but unchanged at the transcriptional level (i.e., the pre-mRNA), were most likely to be affected by the Pacman exoribonuclease. In

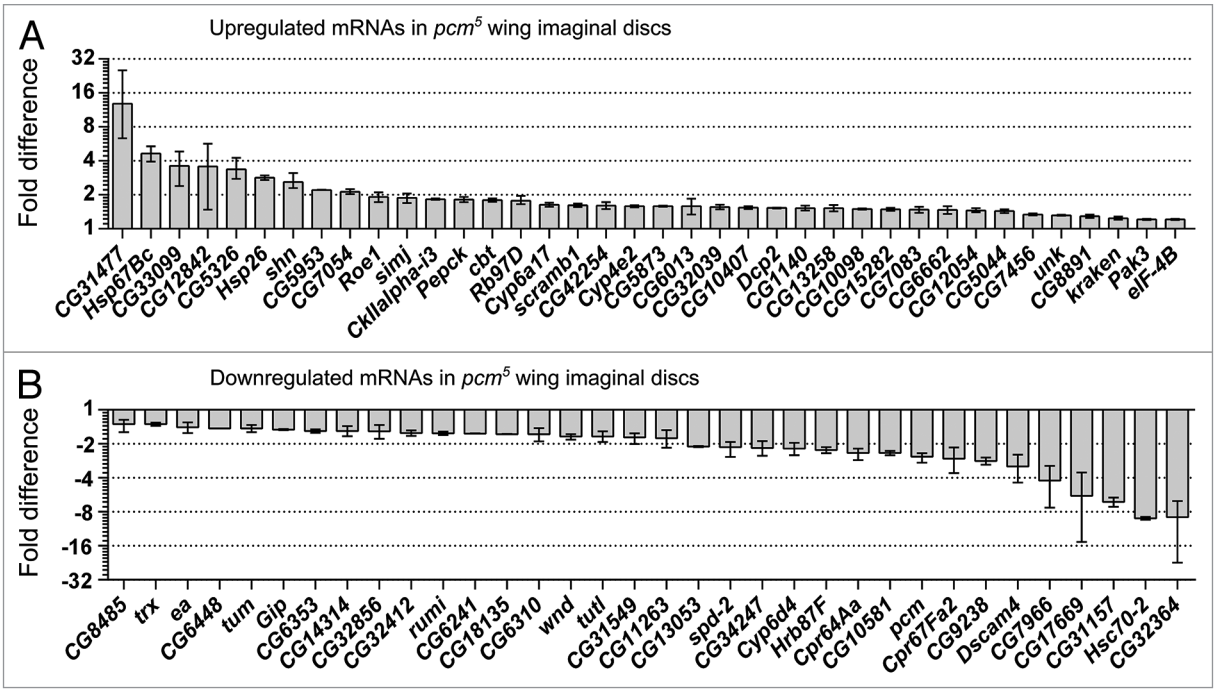


**Figure 3.** Differentially expressed mRNAs in *pcm*$^5$ mutant wing imaginal discs. Affymetrix *Drosophila* Genome 2.0 mRNA microarrays were performed on wild-type and *pcm*$^5$ L3 wing imaginal discs. Thirty-eight genes were found to be upregulated in the *pcm*$^5$ wing imaginal discs, 26 by > 1.5-fold (**A**) and 34 genes were found to be downregulated, 28 by > 1.5-fold (**B**). Normalization was performed using MAS5, RMA and GCRMA. The results from each method were compared and genes that appear in more than one set of results are shown in the figure. Bars represent the mean expression level and error bars show the range.

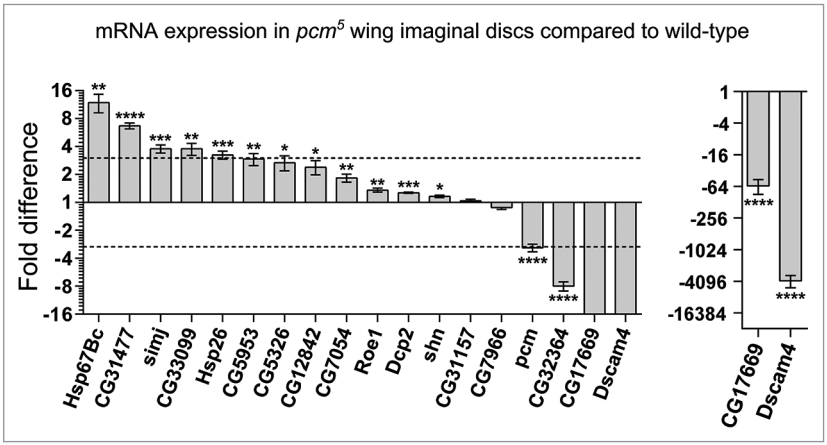


**Figure 4.** Verification of the up/downregulated mRNAs from the microarray results. TaqMan qRT-PCR was used to accurately quantify the expression difference between *pcm*$^5$ and wild-type L3 wing imaginal discs. qRT-PCR was performed on the top 11 upregulated mRNAs, *Dcp2*, the six most downregulated mRNAs and *pacman*. However, *Hsc70-2*, the second most downregulated mRNA from the array results, is not shown on this figure, as the qRT-PCR results were unreliable. For all other mRNAs tested, the qRT-PCR results proved reproducible and showed expression differences comparable to those shown by the microarrays in most cases. However, *CG7699* and *CG31157* were not downregulated when tested by qRT-PCR. Also, *CG17669* and *Dscam4* were downregulated by a much greater extent than was apparent on the arrays. Bars show mean and error bars show standard error. The dashed lines represent a ± 3-fold difference. Stars above the bars indicate significance calculated using a one sample t-test with an expected mean of 1. **** = $P < 0.0001$, *** = $P < 0.001$, ** = $P < 0.01$ and * = $P < 0.05$. n = 11 for *Hsp67Bc*, n = 6 for *CG31477*, *simj*, *CG33099*, *Hsp26*, *CG5953*, *CG7054*, and *CG32364*, n = 5 for *CG5326*, *CG12842*, *Roe1*, and *pcm*, n = 4 for *shn*, *Dcp2*, *CG7966*, *CG31157*, *CG17669*, and *Dscam4*.

contrast, mRNAs that increased in abundance at both the transcriptional level and mRNA level are less likely to be directly affected by Pacman. We measured the pre-mRNA levels of the five mRNAs upregulated by > 3-fold in *pcm*$^5$ mutant; *Hsp67Bc*, *CG31477*, *simjang*, *CG33099* and *Hsp26*, to determine whether Pacman was likely to directly affect these transcripts at the post-transcriptional level. Additionally, we quantified the pre-mRNA levels of *Dcp2*, two mRNAs that did not change level in the *pcm*$^5$ mutant (*CG7699* and *CG31157*), and the three most downregulated mRNAs (*CG32364*, *CG17669*, and *Dscam4*).

Levels of pre-mRNA vs. mRNA were compared in *pcm*$^5$ mutants and wild-type L3 wing imaginal discs. TaqMan qRT-PCR assays were designed to specifically amplify the pre-mRNA transcripts using one of two methods. For *CG31477*, *CG33099*, *simjang*, *CG7966*, *CG31157*, *Dcp2*, *CG32364*, and *Dscam4*, which contain introns, assays were designed against 100 nt sections located within an intron and at least one exon (**Fig. S1**, panels A–G). For *Hsp67Bc*, *Hsp26*, and *CG17669*, which are intronless, assays were designed against the last 50 nt of the 3'UTR plus the following 50 nt of the transcribed RNA, over the polyA cleavage site (**Fig. S1**, panels H–K). The mRNA assays for each gene were the same as those

used previously, with proprietary probe/primer combinations designed across exon-exon boundaries, to ensure specific detection of the mRNA. The TaqMan qRT-PCR assays (mRNA or pre-mRNA) used for genes with more than one mRNA isoform (*CG31477*, *simjang*, *CG31157*, *Dcp2*, and *Dscam4*) were chosen/designed to detect all transcript variants from that gene. The different expression profiles between pre-mRNA and corresponding mature mRNA assays (see below) showed that these methods successfully distinguished between pre-mRNA and mature mRNA. Prior to reverse transcription, all samples were treated with DNase I to prevent the pre-mRNA assays detecting genomic DNA. Controls lacking reverse transcriptase showed that genomic DNA was not detected.

**Figure 5** shows the pre-mRNA compared with the mature mRNA levels of *Hsp67Bc*, *CG31477*, *simjang*, *CG33099*, *Hsp26*, *Dcp2*, *CG7966*, *CG31157*, *CG32364*, *CG17669*, and *Dscam4* in *pcm*$^5$ wing imaginal discs. For *Hsp67Bc*, *CG31477*, *simjang*, and *Hsp26*, the level of pre-mRNA is not significantly different in the mutant compared with wild-type, indicating that the *pcm*$^5$ mutation does not affect the transcription of these mRNAs. However, the levels of mature mRNA are significantly higher in the mutant than in wild-type, showing that Pacman affects these transcripts post-transcriptionally. In contrast, the levels of *CG33099* pre-mRNA and mRNA both increase by approximately the same amount, indicating that the increase in abundance of *CG33099* is due to transcriptional rather than post-transcriptional effects.

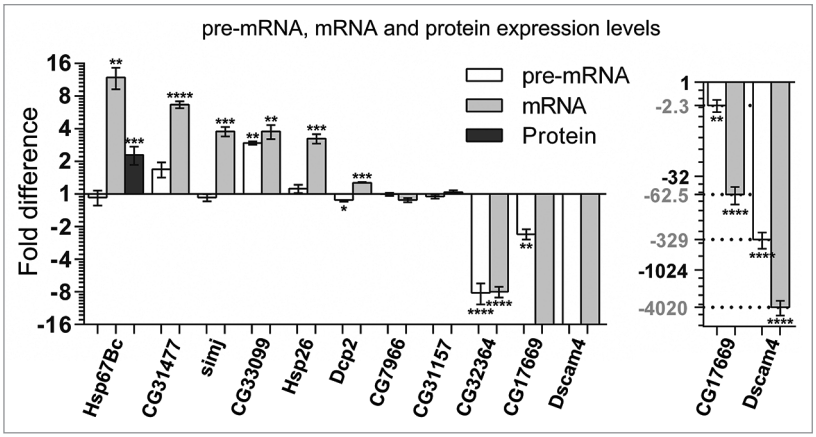


**Figure 5.** Pacman affects some mRNAs at the post-transcriptional level in L3 wing imaginal discs. The pre-mRNA levels were measured for the transcripts upregulated by > 3-fold (*Hsp67Bc*, *CG31477*, *simjang*, *CG33099* and *Hsp26*), three downregulated transcripts (*CG32364*, *CG17669* and *Dscam4*), two unchanged transcripts (*CG7966* and *CG31157*) and *Dcp2*. Bars show mean and error bars show standard error. One sample t-tests were used to test for significance against an expected mean of 1 for each pre-mRNA/mRNA (**** = $p < 0.0001$, *** = $p < 0.001$, ** = $p < 0.01$ and * = $p < 0.05$). The pre-mRNA levels for *Hsp67Bc* (n = 4), *CG31477* (n = 6), *simjang* (n = 6) and *Hsp26* (n = 4) do not differ in the *pcm*$^5$ mutant compared with wild-type, showing that their mRNA levels are affected post-transcriptionally. The level of Hsp67Bc protein (n = 6) increased by 2.3-fold. For *CG33099* (n = 3), the pre-mRNA increases by approximately the same amount as the mature mRNA, showing transcriptional upregulation. Similarly, *CG32364* (n = 4) pre-mRNA decreases by the same amount as the mRNA, showing transcriptional downregulation. *CG17669* (n = 4) and *Dscam4* (n = 4) pre-mRNA levels decreased, showing transcriptional downregulation, but by a much smaller amount than the reduction seen for their mRNAs, suggesting a reduction in transcription was part of, but not the entire explanation for, the reduction of these transcripts. The pre-mRNA and mRNA levels of *CG7966* (n = 4) and *CG31157* (n = 4) were unchanged in the *pcm*$^5$ mutant. The level of *Dcp2* (n = 4) pre-mRNA was significantly reduced, while the mRNA was significantly increased. However, these were very small-scale changes.

Each of the downregulated transcripts (*CG32364, CG17669*, and *Dscam4*) exhibited substantial reductions of transcription in the *pcm*$^5$ mutant. *CG32364* pre-mRNA and mRNA are both reduced by the same amount (8.1-fold and 8.0-fold, respectively), suggesting control of this gene is entirely transcriptional. The levels of pre-mRNA for *CG17669* and *Dscam4* are both greatly reduced, but not to such a great extent as for their corresponding mRNAs, which show a remarkable decrease in abundance (62.5-fold and 4020-fold respectively; **Fig. 5**). This suggests that the downregulation of these mRNAs is not entirely dependent on transcription. However, this is unlikely to be a direct consequence of the *pacman* mutation as we would expect mRNAs directly affected by Pacman to increase in abundance. The mRNA level for *Dcp2* is upregulated 1.3-fold in the *pcm*$^5$ mutant, while its pre-mRNA is 1.1-fold downregulated. Although these changes are statistically significant, they are very small (< 30%) and unlikely to be biologically significant, because a 4-fold increase in Dcp2 protein level (by expression of a transgene) generates no mutant phenotypes when flies are grown under normal conditions.[25] For *CG7966* and *CG31157*, the mRNA levels of which do not change in the *pcm*$^5$ mutant, the pre-mRNA levels also do not change. Since mRNA decay and transcription are often linked,[26] as has been shown for targets of the deadenylases in mammalian cells,[27] then overall mRNA abundance could remain the same if transcripts are stabilized at the same time as transcription is reduced. However, this does not appear to be the case here, as the *pcm*$^5$ mutation results in no change in abundance of these transcripts, either transcriptionally or post-transcriptionally.

**The heat shock protein Hsp67Bc is upregulated in *pcm*$^5$ mutant imaginal discs.** We have shown that the transcripts *Hsp67Bc*, *CG31477*, *simjang*, and *Hsp26* increase post-transcriptionally by at least 3.2-fold in *pcm*$^5$ imaginal discs compared with controls. To have an effect on imaginal disc development these mRNAs would need to be translated into protein. However, the usual pathway for mRNA degradation is thought to be via deadenylation of the transcript, followed by decapping and then degradation by Xrn1/Pacman.[4,12] If this is the case, the decapped transcripts, which would not be optimally translated, would be expected to accumulate. To test whether the accumulated transcripts could be translated, we measured Hsp67Bc and Simjang protein levels using western blot analysis (as far as we are aware, antibodies to CG31477 and *Drosophila* Hsp26 are not available). We were unable to obtain a consistent result using the Simjang antibody, but the Hsp67Bc protein did show a significant increase of around 2.3-fold in *pcm*$^5$ wing imaginal discs (**Fig. 5**), indicating that a portion of the accumulated transcripts can be

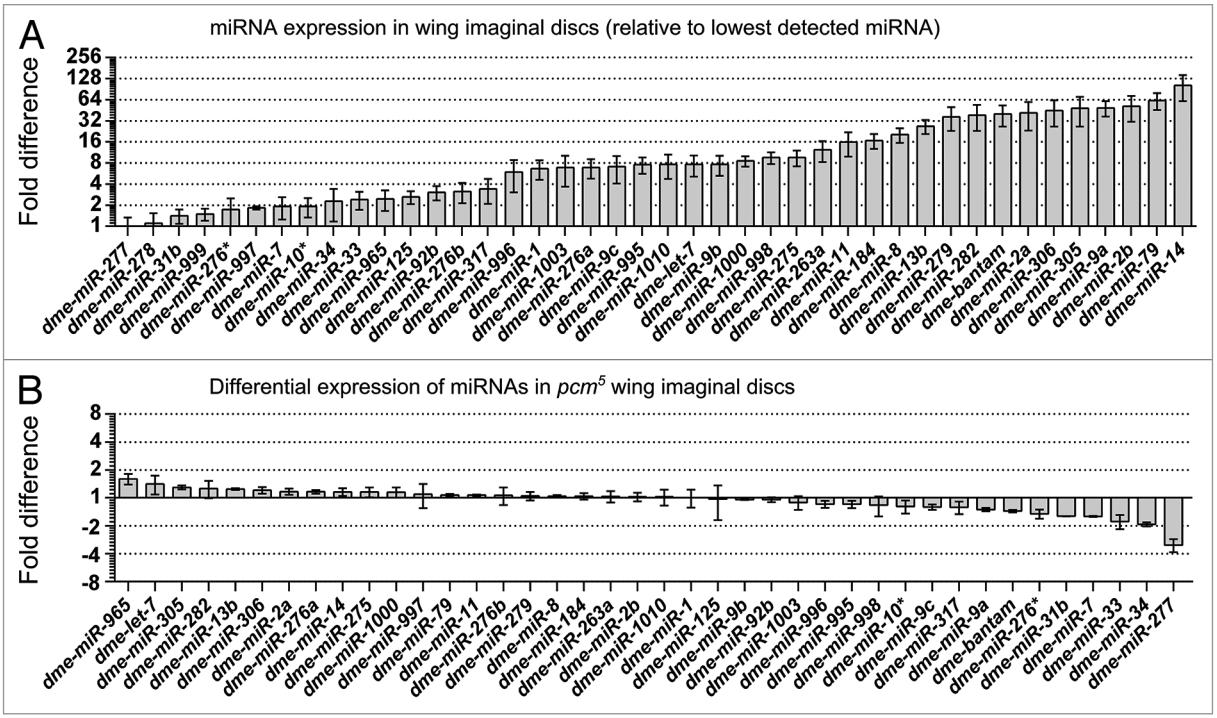


**Figure 6.** Differential expression of miRNAs in *pcm*$^5$ L3 wing imaginal discs compared with wild-type. (**A**) Of 152 miRNAs on the array, 42 were detected above the background level (all were present in both *pcm*$^5$ and wild-type). The most highly expressed, *miR-14-3p*, was at level > 100-fold greater than the level of the lowest level miRNA detected, *miR-277-3p*. Two dual color arrays were performed (*pcm*$^5$ vs. wild-type) and each array contained four spots for each miRNA. Only miRNAs with levels above background in > four spots (out of the eight on the two arrays) were accepted as present. Normalization was performed against six spike-in controls (284 spots in total per array). (**B**) The mean differential expression levels between mutant and wild-type were calculated for each of the detected miRNAs. No miRNA was found to be upregulated by > 2-fold. A single miRNA, *miR-277-3p*, was found to be downregulated by > 2-fold. Error bars show standard error.

translated. Therefore, Hsp67Bc, which is a homolog of HSPB8 in mammals, may contribute to the observed developmental phenotypes.

**Pacman affects the expression of *miR-277-3p* in wing imaginal discs.** One way that Pacman could indirectly regulate the expression of mRNAs would be to control the levels of particular microRNAs, which, in turn, may regulate the abundance of particular transcripts. The role of exoribonucleases in the degradation of miRNAs is a subject that has begun to be addressed in recent years,[2,28-30] with some lines of evidence implicating Pacman/XRN1 in the degradation of at least some miRNAs.[31,32] miRNAs are known to be important at numerous points during *Drosophila* development,[33,34] and the *pcm*$^5$ mutant wing imaginal discs provide an excellent opportunity to test for a link between Pacman and miRNA levels in a system where the reduction of Pacman functionality has observable developmental phenotypes and measurable molecular effects. We reasoned that mature miRNAs that are normally affected by Pacman would increase in the *pcm*$^5$ mutant. In contrast, if Pacman was involved in the processing of a particular pri- or pre-miRNA, then the levels of mature miRNA would be expected to decrease in the *pcm*$^5$ mutant. Alternatively, Pacman may increase or decrease the levels of particular miRNAs via indirect effects on transcription or other gene regulatory events.

To determine the effect of the *pcm*$^5$ mutation on abundance of miRNAs, we used Exiqon LNA miRNA v11.0 "other species" arrays, followed by TaqMan qRT-PCR, to compare the levels of mature miRNAs in *pcm*$^5$ and wild-type L3 wing imaginal discs. For the arrays, 720 wing imaginal discs were dissected from each genotype and divided into two biological replicates. Two dual color arrays were performed and analyzed using GenePix Pro 6.0. Forty-two miRNAs (out of 152 on the array, and 426 in miRBase 19.0) were detected in wild-type *Drosophila* wing imaginal discs. *miR-14-3p* was the most highly expressed miRNA, at a level more than 100-fold higher than that of *miR-277-3p*, the lowest reliably detected miRNA (**Fig. 6**, panel A). Following normalization to spike in controls, the expression levels of individual miRNAs were compared. In the *pcm*$^5$ mutant, there were no miRNAs expressed above 2-fold compared with wild-type, suggesting that, in this case, Pacman is not involved in the degradation of mature miRNAs in *pcm*$^5$ wing imaginal discs (**Fig. 6**, panel B).

The expression levels of the three most downregulated miRNAs, *miR-33-5p*, *miR-34-5p*, and *miR-277-3p*, were verified by Taqman qRT-PCR (n = 4 for each). Two miRNAs that were unchanged on the arrays, *miR-14-3p* and *miR-8-3p*, were also verified by qRT-PCR (n = 4 for each) and did not show a difference in level in *pcm*$^5$ compared with wild-type. *miR-33-5p* and *miR-34-5p* were found to be downregulated in the mutant compared with the wild-type. Although these changes were statistically significant, they were < 2-fold. *miR-277-3p* was downregulated by 5.9-fold in the *pcm*$^5$ wing discs compared with wild-type discs

(**Fig. 7A**). Therefore, Pacman appears to be directly or indirectly involved in expression of this miRNA. To determine whether this effect was at the transcriptional or post-transcriptional level, primers were designed to detect *pri/pre-miR-277* (**Fig. S1**, panel L). *miR-277-3p* and *miR-277-5p* can be processed from *pri/pre-miR-277*, but mature *miR-277-3p* is the overwhelmingly dominant miRNA produced.[35] Comparison of the *pri/pre-miRNA-277* levels with mature *miR-277-3p* levels in *pcm*$^5$ and control wing discs showed that *pri/pre-miRNA-277* was found at similar levels in the mutant and wild-type, whereas the mature *miR-277-3p* was reduced 5.9-fold in *pcm*$^5$ mutant wing imaginal discs (**Fig. 7B**). These data therefore suggest that Pacman affects the maturation of *miR-277-3p*, although it is also possible that this is an indirect effect.

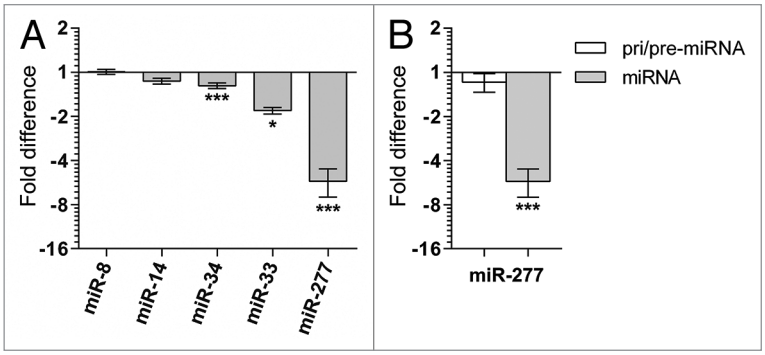


**Figure 7.** (**A**) Validation of miRNA expression differences between wild-type and *pcm*$^5$ L3 wing imaginal discs using TaqMan miRNA qRT-PCR. The three most downregulated miRNAs, *miR-34-5p*, *miR-33-5p*, and *miR-277-3p* were tested along with two miRNAs that did not appear to vary in level, *miR-8-3p* and *miR-14-3p*. One sample t-tests were used to test for significance against an expected mean of 1 for each miRNA (n = 4 for each, **** = $P < 0.0001$, *** = $P < 0.001$, ** = $P < 0.01$, and * = $P < 0.05$, error bars show standard error). (**B**) The decreased level of *miR-277-3p* in *pcm*$^5$ L3 wing imaginal discs occurs post-transcriptionally. The level of *pri/pre-miR-277* was compared with the level of mature *miR-277-3p* in *pcm*$^5$ and wild-type wing discs. The level of *pri/pre-miR-277* in *pcm*$^5$ wing discs was not significantly different from wild-type, suggesting that Pacman affects the biogenesis of this miRNA (n = 7, p = 0.294).

## Discussion

In the present study, we have identified a set of mRNAs and one miRNA that significantly change in abundance upon reduction of expression of the Pacman exoribonuclease in *Drosophila* wing imaginal discs (**Table 1**). Since these RNAs have been identified from wing imaginal discs dissected from developing larvae rather than tissue culture cells, they reflect developmentally important gene expression changes, which occur upon mutation of this exoribonuclease. Developmentally relevant changes in RNA abundance resulting from a reduction in exoribonuclease activity have very rarely been identified so this study represents a significant step forward in understanding the function of the conserved exoribonucleases in vivo. In particular, analysis of the misregulated transcripts identified may start to explain why *pacman* mutant wing imaginal discs and wings are significantly smaller than that of wild-type and how Pacman can influence growth and differentiation.

Surprisingly, our study found relatively few mRNAs that were significantly up or downregulated in abundance in *pcm*$^5$ imaginal discs compared with controls. According to our microarray analysis, followed by validation of these misregulated transcripts by TaqMan qRT-PCR, only eight mRNAs were increased in level by > 2-fold in the *pcm*$^5$ mutant compared with controls (*Hsp67Bc*, *CG31477*, *simjang*, *CG33099*, *Hsp26*, *CG5953*, *CG5326*, and *CG12842*; **Fig. 4**). Of the downregulated transcripts, four (*pacman*, *CG32364*, *CG17669*, and *Dscam4*) were shown by both microarray and TaqMan RT-PCR to be decreased in abundance by > 2-fold. These results are in line with work on the effects of knockdown of the deadenylase subunits Ccr4a (CNOT6) and Ccr4b (CNOT6L) in MCF7 cells where only 79 genes were found to be upregulated (> 1.5-fold) and only four downregulated.[36] Therefore, both studies show that global decay factors affect a surprisingly small number of transcripts.

A possible reason why relatively few transcripts changed in abundance (> 2-fold) in the *pcm*$^5$ mutant is that stabilization of mRNAs by the *pcm*$^5$ mutation is accompanied by a compensatory decrease in transcription and consequently no overall change in the abundance of the majority of mRNAs. This compensatory effect has been seen in studies on the effect of PARN knockdown in mouse myoblasts where the majority of transcripts stabilized were reduced in abundance due to transcriptional control.[27] Other studies in yeast cells have shown that mRNA synthesis and degradation are coupled and that mRNA decay rates are dependent upon events that occur at the promoter.[26,37,38] To determine whether selected transcripts, which did not change in abundance overall, were actually stabilized at the same time as being transcriptionally downregulated, we assessed the levels of pre-mRNA and mRNA of two transcripts, which did not change in overall abundance in the *pcm*$^5$ mutant compared with controls. We found no evidence for substantial reduction of transcription of those mRNAs suggesting that the *pcm*$^5$ mutation does not significantly affect transcription of these mRNAs. Another possibility is that the 3'-5' degradation pathway is upregulated in *pcm*$^5$ mutants, resulting in no change in abundance of many mRNAs. However, we found no evidence for upregulation of transcripts encoding known 3'-5' degradation factors. It is also possible that relatively few transcripts were seen to change in abundance as *pcm*$^5$ is a hypomorphic and not a null mutant. In any case, our experiments aimed to identify the transcripts whose overall expression was substantially perturbed in the *pcm*$^5$ mutant as these transcripts are most likely to result in the biological phenotypes observed. If there is a mechanism to maintain homeostasis in levels of some transcripts then these transcripts are unlikely to cause the mutant phenotype.

The transcripts that significantly increase in abundance in the *pcm*$^5$ mutant could either be due to an increase in transcription, a decrease in decay or a combination of both. By using judiciously placed intronic and exonic primers to distinguish between pre-mRNAs and mRNA we were able to determine whether the *pcm*$^5$ mutation affected these transcripts at the transcriptional and/or post-transcriptional level. As shown in **Figure 5**, the

**Table 1.** Misexpressed RNAs in *pcm*$^5$ wing imaginal discs and their associated molecular and biological functions

| Gene name (Human ortholog) | Fold change in *pcm*$^5$ mutant Pre-mRNA | mRNA | Associated functions (Flybase[43]) | Refs. |
|---|---|---|---|---|
| ***Hsp67Bc*** (*HSPB1-3,6,8, CRYAA, CRYAB*) | -1.1 | **+11.9** ** | **Molecular**: unknown. **Biological:** protein lipidation; response to methotrexate; regulation of translational initiation by eIF2α phosphorylation; regulation of autophagy. | 41,42 |
| ***CG31477*** (*ATP5E*) | +1.7 | **+6.7** **** | **Molecular**: hydrogen-exporting ATPase activity; phosphorylative mechanism. **Biological:** proton transport. | |
| ***simjang*** (*GATAD2A/p66α*) | -1.1 | **+3.8** **** | **Molecular**: protein binding. **Biological:** negative regulation of transcription from RNA polymerase II promoter. | 44,45 |
| ***CG33099*** | **+3.0** ** | **+3.8** ** | **Molecular:** gibberellin 20-oxidase activity. **Biological:** oxidation-reduction process. | |
| ***Hsp26*** (*HSPB1-3,6,8, CRYAA, CRYAB*) | +1.1 | **+3.2** *** | **Molecular**: protein binding. **Biological:** determination of adult lifespan; cold acclimation. | 46 |
| ***CG5953*** | - | **+2.9** ** | **Molecular**: unknown. **Biological:** lateral inhibition. | |
| ***CG5326*** (*ELOVL1,2,4,5,7*) | - | **+2.7** * | **Molecular**: unknown. **Biological**: neurogenesis. | |
| ***CG12842*** | - | **+2.4** * | **Molecular**: unknown. **Biological**: unknown. | |
| ***miR-277-3p*** | -1.2 | **-5.6** *** | **Molecular**: unknown. **Biological:** response to rCGG repeats. | 47 |
| ***CG32364*** | **-8.1** **** | **-8.0** **** | **Molecular**: nucleotide binding; nucleic acid binding. **Biological**: unknown. | |
| ***CG17669*** (*DNAAF3*) | **-2.3** ** | **-62.5** ** | **Molecular**: unknown. **Biological**: unknown. | |
| ***Dscam4*** (multiple, inc. *DSCAM*) | **-328.9** **** | **-4019.3** **** | **Molecular**: identical protein binding. **Biological**: cell adhesion. | 48 |

Underlined transcripts were upregulated post-transcriptionally. Stars below fold change values represent the *P* value (**** = $P < 0.0001$, *** = $P < 0.001$, ** = $P < 0.01$, and * = $P < 0.05$).

levels of *Hsp67Bc*, *CG31477*, *Hsp26*, and *simjang* pre-mRNAs did not increase in the *pcm*$^5$ mutant, but the mature mRNA levels increased significantly. The simplest explanation for this effect is that Pacman normally degrades these mRNAs. However, it is also possible that their increase in abundance is due to an unknown indirect effect. Our results therefore suggest that a limited number of specific transcripts are normally targeted to the 5'-3' degradation machinery for controlled degradation.

Although the above four transcripts are increased in abundance in the *pcm*$^5$ mutant, they would need to be translated to have a phenotypic effect on imaginal disc development. Since it is known that decapping precedes degradation of RNAs by Pacman/Xrn1,[2,12] it would be expected that the upregulated transcripts in the *pcm*$^5$ mutant would be decapped and, therefore, not available for cap-dependent translation. However, our results above show that heat shock protein Hsp67Bc is upregulated 2.3-fold in the *pcm*$^5$ mutant suggesting that at least some of the upregulated *Hsp67Bc* transcripts can be translated. There are at least two possible explanations for this effect. First, it has recently been demonstrated that mRNA decapping is physically coupled to 5'-3' exonucleolytic degradation as Pacman/Xrn1 includes a binding motif for the decapping protein Dcp1 in its C-terminal region (residues 1323–1355 of the 1612aa protein).[19] The *pcm*$^5$ deletion results in loss or disruption of residues 1264–1612 of Pacman, thus removing the Dcp1-binding site. Since removal of the Dcp1-binding domain in Pacman/Xrn1 severely reduces decapping in S2 cells,[19] it is likely that decapping is also inhibited in mutant imaginal disc cells. Second, and additionally, it is possible that the *Hsp67Bc* transcript includes an Internal Ribosome Entry Site (IRES) similar to that of other Heat shock protein transcripts such as *HSP70* in mammalian cells.[39] In this case, the decapped transcripts could be translated by a cap-independent process. The exact mechanism of stabilization of the upregulated transcripts in *pacman* mutants will require further experimentation.

Our experiments also show that the *pcm*$^5$ mutation can result in a remarkable downregulation of a small number of transcripts. *CG32364*, a gene which carries a RNA recognition motif, is downregulated 8-fold at the post-transcriptional level as well as the transcriptional level in *pcm*$^5$ discs, suggesting it is indirectly affected by Pacman. *CG17669* and *Dscam4* are downregulated

62.5-fold and 4020-fold, respectively, in *pcm*$^5$ discs due to both transcriptional and post-transcriptional effects. The reasons for these decreases are not clear but could be due to Pacman directly or indirectly upregulating a transcriptional repressor. Alternatively, this could be a result of reduction of a specific cell population expressing Dscam4 and/or CG17669.

Our study also shows that the *pcm*$^5$ mutation affects the levels of mature *miR-277-3p* in wing imaginal discs. The decrease in levels of mature *miR-277-3p* in imaginal discs of the *pcm*$^5$ mutant is interesting as it is the first time that this 5'-3' exoribonuclease has been shown to specifically affect the expression levels of a miRNA in *Drosophila*. This mature miRNA was downregulated 5.9-fold in the *pcm*$^5$ mutant while the levels of its pri-and pre-miRNAs were unchanged between mutant and control. Therefore, it appears that Pacman can affect the processing of *miR-277-3p*, perhaps in a similar manner to that observed for *miR-34-5p* in *Drosophila* S2 cells where the 3'-to-5' exoribonuclease Nibbler trims miRNAs bound to Ago1.[40] However, it is also possible that this effect is indirect, in that this miRNA may normally be protected from degradation by binding to its target mRNA (target-mediated miRNA protection).[32] In this case, the downregulation of one or more of the transcripts in the *pcm*$^5$ mutant could result in acceleration of *miR-277-3p* decay. Although it is presently unclear how Pacman could affect the expression of this miRNA, the processing/degradation of this miRNA must be specific, as it is the only one out of the 42 mature miRNAs detected in wing discs that is regulated in this way.

How could the changes in abundance of these misregulated mRNAs and miRNA in the *pcm*$^5$ mutant affect growth and differentiation of imaginal discs? A summary of the RNAs misregulated in the *pcm*$^5$ mutant are listed in **Table 1**, together with their proposed functions. A striking function of the most upregulated transcript (*Hsp67Bc*) is its involvement in autophagy. Hsp67Bc has recently been shown to be the functional ortholog of human HSPB8 (Hsp22), which induces autophagy via the eIF2α pathway.[41,42] The higher levels of Hsp67Bc protein observed in *pcm*$^5$ mutant wing discs compared with controls could be reducing imaginal disc growth by decreasing protein synthesis and/or inducing autophagy. The significant reduction of expression of *miR-277-3p* in *pcm*$^5$ mutant discs suggests another way in which Pacman may affect the growth of discs. If *miR-277-3p* targets mRNAs encoding proteins involved in growth inhibition, then a decrease in this miRNA could lead to a reduction in size of mutant imaginal discs. Although we checked the levels of some of the proteins encoded by putative mRNA targets of *miR-277-3p* we could not find any evidence for changes in expression. Therefore, the molecular pathways controlled by *miR-277-3p* in imaginal disc development will require further experimental work. Since Pacman/Xrn1 is highly conserved in all eukaryotes, these investigations are likely to shed light on autophagy and apoptosis control in all multicellular organisms.

## Materials and Methods

**Fly stocks.** Fly stocks were cultivated on standard media at 25 °C in uncrowded conditions. Creation of the *pcm*$^5$ allele was previously described by Grima et al.[20] The wild-type stock used was created by a neutral excision of the P-element used to create *pcm*$^5$ (*P{EP}EP1526*, stock 11456 from Bloomington Stock Center). A 43 bp "footprint" was left by the P-element in the intron of *CG43260*.

**Measurement of wing and wing disc size.** For size measurements, wing imaginal discs were dissected from L3 larvae and an individual image was taken using a dissecting microscope at a constant magnification. The area each disc was then measured in arbitrary units using ImageJ (www.rsbweb.nih.gov/ij/). For images, L3 wing imaginal discs were dissected and mounted in 85% glycerol under a size 1 coverslip, with an additional size one coverslip cut in half and placed at each side of the area containing the imaginal discs to act as spacers. Images were produced using Axiovision 4.7 on an Axioplan microscope (Carl Zeiss). Wings were mounted in DPX medium (Fischer Scientific, Cat. no. 10050080) under a size 0 coverslip (weighted down overnight).

**Molecular techniques.** RNA extractions were performed using an RNeasy Mini Kit (Qiagen, Cat. no. 74104) or a *miR*Vana miRNA isolation kit (Life Technologies, Cat. no. AM1560). The *miR*Vana kit was used for total RNA extraction when RNAs < 200 nt (miRNAs etc.) were required. Samples were treated with a DNA-*free* kit (Life Technologies, Cat. no. AM1906) and their concentrations were measured on a NanoDrop 1000 spectrophotometer (Thermo Scientfic). For the *Drosophila* Genome 2.0 mRNA microarrays (Affymetrix, Cat. no. 900531), wing imaginal disc samples were homogenized in RLT buffer from the RNeasy Mini kit with β-mercaptoethanol added before being sent on dry ice to the Sir Henry Wellcome Functional Genomics Facility (University of Glasgow). For the LNA miRNA v11.0 "other species" arrays (Exiqon, Cat. no. 208213-A), the samples were labeled with either Hy5 or Hy3 dyes in the supplied labeling kit (Cat. no. 208032-A). A miRCURY LNA Array Spike-in miRNA kit (Exiqon, Cat. no. 208040) was also used. Hybridization was performed in Microarray Hybridization chambers (Agilent) in a rotary HB-1000 hybridization oven (UVP) at 65 °C. The arrays were scanned using an Axon GenePix 4000B Microarray Scanner (Molecular Devices) and analyzed using GenePix Pro 6.0 (Molecular Devices). Normalization was performed using the spike in miRNAs.

For qRT-PCR, cDNA was prepared from the RNA samples using a High Capacity cDNA Reverse Transcription Kit (Life Technologies, Cat. no. 4368814) for mRNA/pre-mRNA or a TaqMan microRNA Reverse Transcription Kit (Life Technologies, Cat. no. 4366596) for miRNAs. Specific primers (supplied) were used for each miRNA RT reaction, and random primers were used for the mRNA/pre-mRNA RT reactions. qRT-PCR was performed on the cDNA produced from either RT protocol using TaqMan Universal PCR Master Mix, No AmpErase UNG (Life Technologies, Cat. no. 4324018) and an appropriate TaqMan mRNA/miRNA assay (Life Technologies). All mRNA and miRNA TaqMan assays used were pre-designed. For custom pre-mRNA assays, 100 nt of sequence of the desired target area was submitted to Life Technologies' web-based Custom TaqMan Assay Design Tool (**Fig. S1**).

Western blotting was performed on samples containing 60 wing imaginal discs. Tubulin was used as an internal control. Mouse

anti-Tubulin primary antibody (Sigma, Cat. no. T9026) was used at a 1:2,000 dilution with an anti-mouse-HRP conjugated secondary antibody (Sigma, Cat. no. A2304) at 1:80000. Hsp67Bc primary antibody was used at a 1:1,000 dilution with an anti-rabbit-HRP conjugated secondary antibody at 1:80000 (Sigma, Cat. no. A0545). Antibody binding was detected using Amersham ECL detection reagents (GE Healthcare, Cat. no. RPN2209). Relative quantification of bands was performed in ImageJ.

### Disclosure of Potential Conflicts of Interest

No potential conflicts of interest were disclosed.

### Acknowledgments

The authors would like to thank Clare Rizzo-Singh, Karen Scruby and Ben Towler for technical help. We would also like to thank Julie Aspden and Simon Morley for checking the manuscript and for helpful comments. Rabbit Hsp67Bc primary antibody was kindly provided by Dr Serena Carra (University of Modena and Reggio Emilia). This work was funded by the Biotechnology and Biological Sciences Research Council (grants BB/I021345/1 and BB/G002754/1), an MRC studentship (to JAW) and a Junior Research Associate Summer studentship from the University of Sussex (to HNP).

### Supplemental Materials

Supplemental materials may be found here:
www.landesbioscience.com/journals/rnabiology/article/25354

### References

1. Cheadle C, Fan J, Cho-Chung YS, Werner T, Ray J, Do L, et al. Control of gene expression during T cell activation: alternate regulation of mRNA transcription and mRNA stability. BMC Genomics 2005; 6:75; PMID:15907206; http://dx.doi.org/10.1186/1471-2164-6-75
2. Jones CI, Zabolotskaya MV, Newbury SF. The 5'→3' exoribonuclease XRN1/Pacman and its functions in cellular processes and development. Wiley Interdiscip Rev RNA 2012; 3:455-68; PMID:22383165; http://dx.doi.org/10.1002/wrna.1109
3. Baou M, Jewell A, Murphy JJ. TIS11 family proteins and their roles in posttranscriptional gene regulation. J Biomed Biotechnol 2009; 2009:634520; PMID:19672455; http://dx.doi.org/10.1155/2009/634520
4. Garneau NL, Wilusz J, Wilusz CJ. The highways and byways of mRNA decay. Nat Rev Mol Cell Biol 2007; 8:113-26; PMID:17245413; http://dx.doi.org/10.1038/nrm2104
5. Newbury SF. Control of mRNA stability in eukaryotes. Biochem Soc Trans 2006; 34:30-4; PMID:16246172; http://dx.doi.org/10.1042/BST0340030
6. Carballo E, Blackshear PJ. Roles of tumor necrosis factor-alpha receptor subtypes in the pathogenesis of the tristetraprolin-deficiency syndrome. Blood 2001; 98:2389-95; PMID:11588035; http://dx.doi.org/10.1182/blood.V98.8.2389
7. Carballo E, Lai WS, Blackshear PJ. Evidence that tristetraprolin is a physiological regulator of granulocyte-macrophage colony-stimulating factor messenger RNA deadenylation and stability. Blood 2000; 95:1891-9; PMID:10706852
8. Stoecklin G, Tenenbaum SA, Mayo T, Chittur SV, George AD, Baroni TE, et al. Genome-wide analysis identifies interleukin-10 mRNA as target of tristetraprolin. J Biol Chem 2008; 283:11689-99; PMID:18256032; http://dx.doi.org/10.1074/jbc.M709657200
9. Newbury SF, Woollard AC. The 5'-3' exoribonuclease xrn-1 is essential for ventral epithelial enclosure during *C. elegans* embryogenesis. RNA 2004; 10:59-65; PMID:14681585; http://dx.doi.org/10.1261/rna.2195504
10. Parker R, Song H. The enzymes and control of eukaryotic mRNA turnover. Nat Struct Mol Biol 2004; 11:121-7; PMID:14749774; http://dx.doi.org/10.1038/nsmb724
11. Till DD, Linz B, Seago JE, Elgar SJ, Marujo PE, Elias ML, et al. Identification and developmental expression of a 5'-3' exoribonuclease from *Drosophila melanogaster*. Mech Dev 1998; 79:51-5; PMID:10349620; http://dx.doi.org/10.1016/S0925-4773(98)00173-7
12. Nagarajan VK, Jones CI, Newbury SF, Green PJ. XRN 5'→3' exoribonucleases: Structure, mechanisms and functions. Biochim Biophys Acta 2013; 1829:590-603; PMID:23517755; http://dx.doi.org/10.1016/j.bbagrm.2013.03.005
13. Orban TI, Izaurralde E. Decay of mRNAs targeted by RISC requires XRN1, the Ski complex, and the exosome. RNA 2005; 11:459-69; PMID:15703439; http://dx.doi.org/10.1261/rna.7231505
14. Kulkarni M, Ozgur S, Stoecklin G. On track with P-bodies. Biochem Soc Trans 2010; 38:242-51; PMID:20074068; http://dx.doi.org/10.1042/BST0380242
15. Zabolotskaya MV, Grima DP, Lin MD, Chou TB, Newbury SF. The 5'-3' exoribonuclease Pacman is required for normal male fertility and is dynamically localized in cytoplasmic particles in *Drosophila* testis cells. Biochem J 2008; 416:327-35; PMID:18652574; http://dx.doi.org/10.1042/BJ20071720
16. Reijns MA, Alexander RD, Spiller MP, Beggs JD. A role for Q/N-rich aggregation-prone regions in P-body localization. J Cell Sci 2008; 121:2463-72; PMID:18611963; http://dx.doi.org/10.1242/jcs.024976
17. Jinek M, Coyle SM, Doudna JA. Coupled 5' nucleotide recognition and processivity in Xrn1-mediated mRNA decay. Mol Cell 2011; 41:600-8; PMID:21362555; http://dx.doi.org/10.1016/j.molcel.2011.02.004
18. Davey NE, Cowan JL, Shields DC, Gibson TJ, Coldwell MJ, Edwards RJ. SLiMPrints: conservation-based discovery of functional motif fingerprints in intrinsically disordered protein regions. Nucleic Acids Res 2012; 40:10628-41; PMID:22977176; http://dx.doi.org/10.1093/nar/gks854
19. Braun JE, Truffault V, Boland A, Huntzinger E, Chang CT, Haas G, et al. A direct interaction between DCP1 and XRN1 couples mRNA decapping to 5' exonucleolytic degradation. Nat Struct Mol Biol 2012; 19:1324-31; PMID:23142987; http://dx.doi.org/10.1038/nsmb.2413
20. Grima DP, Sullivan M, Zabolotskaya MV, Browne C, Seago J, Wan KC, et al. The 5'-3' exoribonuclease *pacman* is required for epithelial sheet sealing in *Drosophila* and genetically interacts with the phosphatase *puckered.* Biol Cell 2008; 100:687-701; PMID:18547166; http://dx.doi.org/10.1042/BC20080049
21. Bate M, Arias AM. The embryonic origin of imaginal discs in *Drosophila.* Development 1991; 112:755-61; PMID:1935688
22. Irizarry RA, Hobbs B, Collin F, Beazer-Barclay YD, Antonellis KJ, Scherf U, et al. Exploration, normalization, and summaries of high density oligonucleotide array probe level data. Biostatistics 2003; 4:249-64; PMID:12925520; http://dx.doi.org/10.1093/biostatistics/4.2.249
23. Hubbell E, Liu WM, Mei R. Robust estimators for expression analysis. Bioinformatics 2002; 18:1585-92; PMID:12490442; http://dx.doi.org/10.1093/bioinformatics/18.12.1585
24. Wu ZJ, Irizarry RA, Gentleman R, Martinez-Murillo F, Spencer F. A model-based background adjustment for oligonucleotide expression arrays. J Am Stat Assoc 2004; 99:909-17; http://dx.doi.org/10.1198/016214504000000683
25. Ren J, Sun J, Zhang Y, Liu T, Ren Q, Li Y, et al. Down-regulation of Decapping Protein 2 mediates chronic nicotine exposure-induced locomotor hyperactivity in *Drosophila.* PLoS One 2012; 7:e52521; PMID:23300696; http://dx.doi.org/10.1371/journal.pone.0052521
26. Dori-Bachash M, Shema E, Tirosh I. Coupled evolution of transcription and mRNA degradation. PLoS Biol 2011; 9:e1001106; PMID:21811398; http://dx.doi.org/10.1371/journal.pbio.1001106
27. Lee JE, Lee JY, Trembly J, Wilusz J, Tian B, Wilusz CJ. The PARN deadenylase targets a discrete set of mRNAs for decay and regulates cell motility in mouse myoblasts. PLoS Genet 2012; 8:e1002901; PMID:22956911; http://dx.doi.org/10.1371/journal.pgen.1002901
28. Kai ZS, Pasquinelli AE. MicroRNA assassins: factors that regulate the disappearance of miRNAs. Nat Struct Mol Biol 2010; 17:5-10; PMID:20051982; http://dx.doi.org/10.1038/nsmb.1762
29. Zhang Z, Qin YW, Brewer G, Jing Q. MicroRNA degradation and turnover: regulating the regulators. Wiley Interdiscip Rev RNA 2012; 3:593-600; PMID:22461385; http://dx.doi.org/10.1002/wrna.1114
30. Chang HM, Triboulet R, Thornton JE, Gregory RI. A role for the Perlman syndrome exonuclease Dis3l2 in the Lin28-let-7 pathway. Nature 2013; 497:244-8; PMID:23594738; http://dx.doi.org/10.1038/nature12119
31. Bail S, Swerdel M, Liu H, Jiao X, Goff LA, Hart RP, et al. Differential regulation of microRNA stability. RNA 2010; 16:1032-9; PMID:20348442; http://dx.doi.org/10.1261/rna.1851510
32. Chatterjee S, Fasler M, Büssing I, Grosshans H. Target-mediated protection of endogenous microRNAs in *C. elegans.* Dev Cell 2011; 20:388-96; PMID:21397849; http://dx.doi.org/10.1016/j.devcel.2011.02.008
33. Waldron JA, Newbury SF. The roles of miRNAs in wing imaginal disc development in Drosophila. Biochem Soc Trans 2012; 40:891-5; PMID:22817754; http://dx.doi.org/10.1042/BST20120035
34. Jones CI, Newbury SF. Functions of microRNAs in *Drosophila* development. Biochem Soc Trans 2010; 38:1137-43; PMID:20659018; http://dx.doi.org/10.1042/BST0381137

35. Kozomara A, Griffiths-Jones S. miRBase: integrating microRNA annotation and deep-sequencing data. Nucleic Acids Res 2011; 39(Database issue):D152-7; PMID:21037258; http://dx.doi.org/10.1093/nar/gkq1027
36. Mittal S, Aslam A, Doidge R, Medica R, Winkler GS. The Ccr4a (CNOT6) and Ccr4b (CNOT6L) deadenylase subunits of the human Ccr4-Not complex contribute to the prevention of cell death and senescence. Mol Biol Cell 2011; 22:748-58; PMID:21233283; http://dx.doi.org/10.1091/mbc.E10-11-0898
37. Shalem O, Groisman B, Choder M, Dahan O, Pilpel Y. Transcriptome kinetics is governed by a genome-wide coupling of mRNA production and degradation: a role for RNA Pol II. PLoS Genet 2011; 7:e1002273; PMID:21931566; http://dx.doi.org/10.1371/journal.pgen.1002273
38. Sun M, Schwalb B, Schulz D, Pirkl N, Etzold S, Larivière L, et al. Comparative dynamic transcriptome analysis (cDTA) reveals mutual feedback between mRNA synthesis and degradation. Genome Res 2012; 22:1350-9; PMID:22466169; http://dx.doi.org/10.1101/gr.130161.111
39. Rocchi L, Alfieri RR, Petronini PG, Montanaro L, Brigotti M. 5'-Untranslated region of heat shock protein 70 mRNA drives translation under hypertonic conditions. Biochem Biophys Res Commun 2013; 431:321-5; PMID:23291172; http://dx.doi.org/10.1016/j.bbrc.2012.12.100
40. Han BW, Hung JH, Weng Z, Zamore PD, Ameres SL. The 3'-to-5' exoribonuclease Nibbler shapes the 3' ends of microRNAs bound to Drosophila Argonaute1. Curr Biol 2011; 21:1878-87; PMID:22055293; http://dx.doi.org/10.1016/j.cub.2011.09.034
41. Carra S, Boncoraglio A, Kanon B, Brunsting JF, Minoia M, Rana A, et al. Identification of the *Drosophila* ortholog of HSPB8: implication of HSPB8 loss of function in protein folding diseases. J Biol Chem 2010; 285:37811-22; PMID:20858900; http://dx.doi.org/10.1074/jbc.M110.127498
42. Carra S, Brunsting JF, Lambert H, Landry J, Kampinga HH. HspB8 participates in protein quality control by a non-chaperone-like mechanism that requires eIF2α phosphorylation. J Biol Chem 2009; 284:5523-32; PMID:19114712; http://dx.doi.org/10.1074/jbc.M807440200
43. McQuilton P, St Pierre SE, Thurmond J; FlyBase Consortium. FlyBase 101--the basics of navigating FlyBase. Nucleic Acids Res 2012; 40(Database issue):D706-14; PMID:22127867; http://dx.doi.org/10.1093/nar/gkr1030
44. Kon C, Cadigan KM, da Silva SL, Nusse R. Developmental roles of the Mi-2/NURD-associated protein p66 in Drosophila. Genetics 2005; 169:2087-100; PMID:15695365; http://dx.doi.org/10.1534/genetics.104.034595
45. Kim YO, Park SJ, Balaban RS, Nirenberg M, Kim Y. A functional genomic screen for cardiogenic genes using RNA interference in developing *Drosophila* embryos. Proc Natl Acad Sci USA 2004; 101:159-64; PMID:14684833; http://dx.doi.org/10.1073/pnas.0307205101
46. Tower J. Heat shock proteins and *Drosophila* aging. Exp Gerontol 2011; 46:355-62; PMID:20840862; http://dx.doi.org/10.1016/j.exger.2010.09.002
47. Tan H, Poidevin M, Li H, Chen D, Jin P. MicroRNA-277 modulates the neurodegeneration caused by Fragile X premutation rCGG repeats. PLoS Genet 2012; 8:e1002681; PMID:22570635; http://dx.doi.org/10.1371/journal.pgen.1002681
48. Armitage SAO, Freiburg RY, Kurtz J, Bravo IG. The evolution of Dscam genes across the arthropods. BMC Evol Biol 2012; 12:53; PMID:22500922; http://dx.doi.org/10.1186/1471-2148-12-53